Pergamon

Available online at www.sciencedirect.com
SCIENCE DIRECT®

Cement and Concrete Research 33 (2003) 1837–1849

CEMENT AND CONCRETE RESEARCH

Influence of aggregate size, water cement ratio and age on the microstructure of the interfacial transition zone

Amir Elsharief, Menashi D. Cohen*, Jan Olek

School of Civil Engineering, Purdue University, 1284 Civil Engineering Building, G217, West Lafayette, IN 47907, USA

Received 20 September 2002; accepted 11 June 2003

Abstract

This paper presents the results of an investigation on the effect of water–cement ratio (w/c), aggregate size, and age on the microstructure of the interfacial transition zone (ITZ) between normal weight aggregate and the bulk cement paste. Backscattered electron images (BSE) obtained by scanning electron microscope were used to characterize the ITZ microstructure. The results suggest that the w/c plays an important role in controlling the microstructure of the ITZ and its thickness. Reducing w/c from 0.55 to 0.40 resulted in an ITZ with characteristics that are not distinguishable from those of the bulk paste as demonstrated by BSE images. Aggregate size appears to have an important influence on the ITZ characteristics. Reducing the aggregate size tends to reduce the ITZ porosity. The evolution of the ITZ microstructure relative to that of the bulk paste appears to depend on the initial content of the unhydrated cement grains (UH). The results suggest that the presence of a relatively low amount of UH in the ITZ at early age may cause the porosity of the ITZ, relative to that of the bulk paste, to increase with time. The presence of relatively large amount of UH in the ITZ at early ages may cause its porosity, relative to that of the bulk paste, to decrease with time.

Keywords: Interfacial transition zone; SEM; Backscattered electron imaging; Image analysis; Microstructure

1. Introduction

It is well established that the interfacial transition zone (ITZ) between aggregate and cement paste has a different microstructure than the bulk paste [1–5]. The microstructure of the ITZ has been characterized mainly by using backscattered electron images (BSE) obtained by the scanning electron microscopy (SEM). Among the reported characteristics of the ITZ are its higher porosity and lower content of unhydrated cement grains (UH) as compared to the bulk paste. These properties change as a function of distance from aggregate surface until they gradually converge to the levels of properties observed in the bulk paste. The distance over which this gradient of properties exists has been defined as the ITZ thickness. It has been suggested that the ITZ thickness, as well as its microstructure, is controlled mainly by the wall effect [6,7]. This implies that the cement grain size distribution is an important factor controlling the ITZ characteristics. Water–cement ratio (w/c) has been considered to have only small effect on the ITZ microstructure [6].

The influence of the aggregate size on the ITZ characteristics has not received much attention. Ping et al. [8] attempted to clarify the effect of the aggregate size by using electrical conductivity method. To the authors' knowledge there is no report on the quantitative effect of the aggregate size on the ITZ microstructure.

In a study conducted by Diamond and Huang [9] it was suggested that the ITZ microstructure in not much different than that of the bulk paste and that the mixing procedure has a strong impact on its characteristics. This particular study concluded that the ITZ formation was primarily due to the bleeding around the aggregate and suggested that if the bleeding can be eliminated by efficient mixing, then the resulting ITZ microstructure will hardly be different than that of the bulk paste.

The objective of the present study is to investigate the effect of w/c and aggregate size on the ITZ characteristics and to compare the evolution of the ITZ microstructure to that of the bulk paste using the BSE of the ITZ and the bulk paste. The quantitative information used to characterize the ITZ and the bulk paste was derived from backscattered

* Corresponding author. Tel.: +1-765-494-5018; fax: +1-765-496-1364.
E-mail address: mcohen@ecn.purdue.edu (M.D. Cohen).

0008-8846/$ – see front matter © 2003 Elsevier Ltd. All rights reserved.
doi:10.1016/S0008-8846(03)00205-9

images, which were processed using image analysis software. The parameters used for characterization and comparison purposes were detectable porosity and UH.

2. Experimental

2.1. Materials, mixing and casting

Two sets of mortar specimens were prepared, one with a w/c of 0.55 and the other with a w/c of 0.40. ASTM type I cement was used. The sand used for mortar preparation was comprised mainly of granite and quartzite. Two aggregate sizes were used: 2.36–4.75 mm (passing #4 and retained on #8 standard sieve) and 150–300 μm (passing #50 and retained on #100). These two sizes of aggregate were blended together prior to mixing at the proportions shown in Table 1a. The total aggregate content and the amount of each size was adjusted to get a mortar flow of approximately 105% using standard flow table conforming to ASTM C 230 and following the procedure outlined in ASTM C1437. The mixture proportions used are given in Table 1b. The volume fraction of cement paste was kept constant at 50% of the total mixture volume for all mixtures. All mortars were mixed in a Hobart mortar mixer with 13,500-ml capacity. Mixing was done according to the procedure described in ASTM C 305 except that the time for the last mixing interval was increased from 1 to 4 min.

After mixing, the mortar was placed in a $1 \times 1 \times 12$-in. horizontal molds, consolidated by rodding and finished. After finishing the molds were covered with wet burlap and kept in the laboratory for 24 h. After 24 h, the specimens were demolded and placed in a saturated limewater solution until the day of testing.

Table 1
Mortar mixture composition

W/C	#4–8 (vol. %)	#50–100 (vol. %)
(a) Aggregate proportions of the two gradations used in mortar mixtures		
0.55	10	40
0.40	30	20

(b) Mix proportions for w/c of 0.55 and 0.40 mortars	
w/c	0.55
Sand volume (%)	50
Sand weight (kg/m^3)	1325
Cement (kg/m^3)	576
Water (kg/m^3)	317
2.36- to 4.75-mm (#4–8) aggregate (kg/m^3)	265
150- to 300-μm (#50–100) aggregate (kg/m^3)	1060
w/c	0.40
Sand volume (%)	50
Sand weight (kg/m^3)	1325
Cement (kg/m^3)	696.9
Water (kg/m^3)	278.7
2.36- to 4.75-mm (#4–8) aggregate (kg/m^3)	795
150- to 300-μm (#50–100) aggregate (kg/m^3)	530

2.2. Specimen preparation for SEM analysis

Periodically the specimens were removed from the limewater and small sample was cut off using an electric saw. These small samples were placed in an oven at 50 °C for 1 week to remove the free water. The specimens reached constant weight within the 7-day drying period, which indicated that most of the free water had evaporated. Drying at this temperature did not appear to cause cracking. Upon the completion of drying the specimens were placed in plastic molds and vacuum saturated with low viscosity epoxy for 4 h and subsequently placed in an oven set at 70 °C to cure the epoxy. After the epoxy was fully cured, one face of the specimen was exposed by using a precision saw cooled with propylene glycol and operated at low speed. The exposed face was ground and polished using cloth impregnated with diamond paste of successively finer sizes down to 0.25 μm.

2.3. Image acquisition and results

The polished specimens were examined in the backscattered mode using an R.J. Lee Personal Scanning Electron microscope. Analysis was performed around randomly selected aggregate particles. A particular aggregate was selected for analysis by moving the SEM stage in one direction, starting from the specimen edge, for a specified period of time. The aggregate particle in the center of the image obtained at $\times 100$ magnification was selected for the analysis.

The procedure used by Diamond and Huang [9] and Diamond [10] in acquiring the image was adopted in this study. This technique consisted of obtaining BSE for the entire ITZ surrounding the selected aggregate. It was a simple task to distinguish between the two groups of aggregate used in this study due to the large difference in their sizes. It typically took approximately 45–60 images to cover the ITZ around a 2.36- to 4.75-mm aggregate (#4–8), while the typical number of images for a 150- to 300-μm aggregate (#50–100) was 4–6 images. BSE images were also obtained in the bulk paste at least 50 μm from the aggregate surface.

The total number of images obtained for the ITZ and the bulk paste was based on the statistical consideration that the average value of the feature studied should be within 10% of the true average using 95% confidence interval and assuming normal distribution. An example of the statistical analysis is provided in Appendix A. All the images were taken at $\times 500$ magnification and had 512×512 pixels resolution. Based on this resolution the minimum size of a recognizable feature had to be 0.34 μm. The Strips of 10-

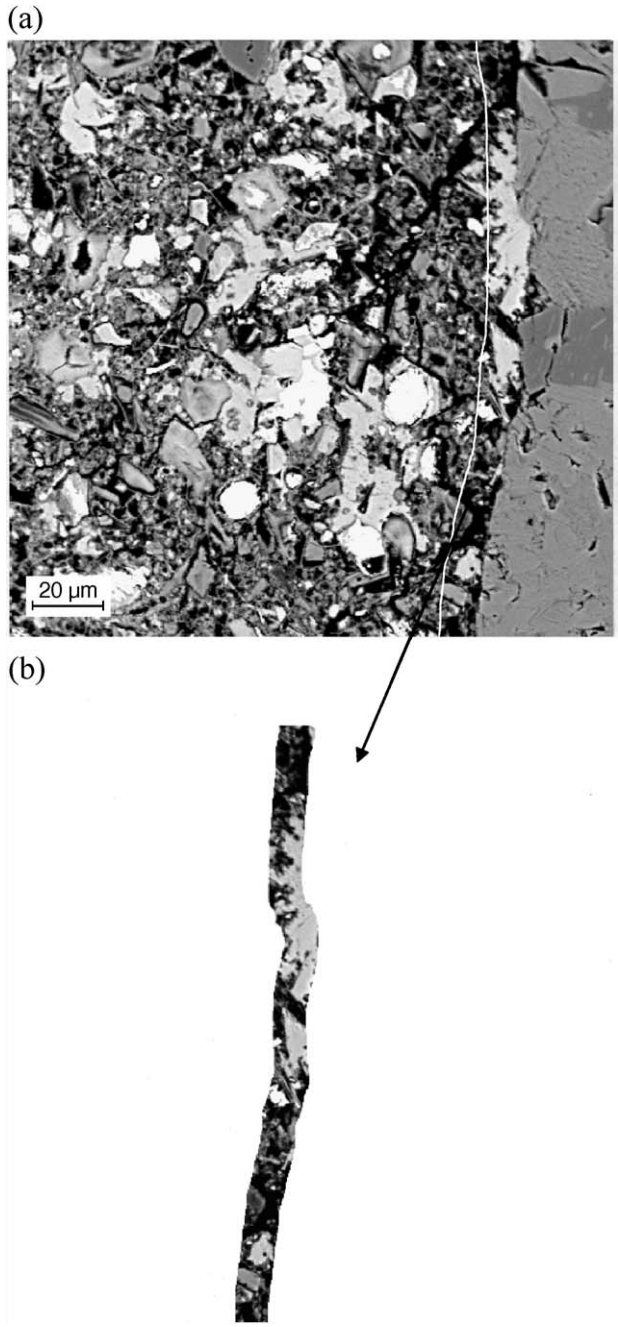

Fig. 1. (a) Paste around #4–8 aggregate in 7-day old mortar with w/c 0.55 at 7-day age; (b) 10-μm strip isolated "cut" from the immediate vicinity of the aggregate.

μm wide were successively cut from the image starting at the aggregate surface and up to 40 μm away from the aggregate surface, as illustrated in Fig. 1. These strips were approximately 175 μm long. The ITZ thickness was previously reported to be around 20–50 μm [4,6]. Thus, it was decided to analyze the strips located up to 40 μm from the aggregate surface to obtain meaningful information about the ITZ characteristics.

The bulk paste images were taken randomly at spots, which were at least 50 μm away from the nearest aggregate. The dimensions of these images were of 175 × 175 μm and they were analyzed as a whole area without separating it into individual strips.

The ITZ strips and the bulk paste images were analyzed using Image Pro software. The images were segmented based on the grey level of the different features selected for analysis. The two features selected for segmentation were the percent of detectable porosity and percent of UH. The grey level limits for each feature were determined after carefully examining a number of images to make certain the

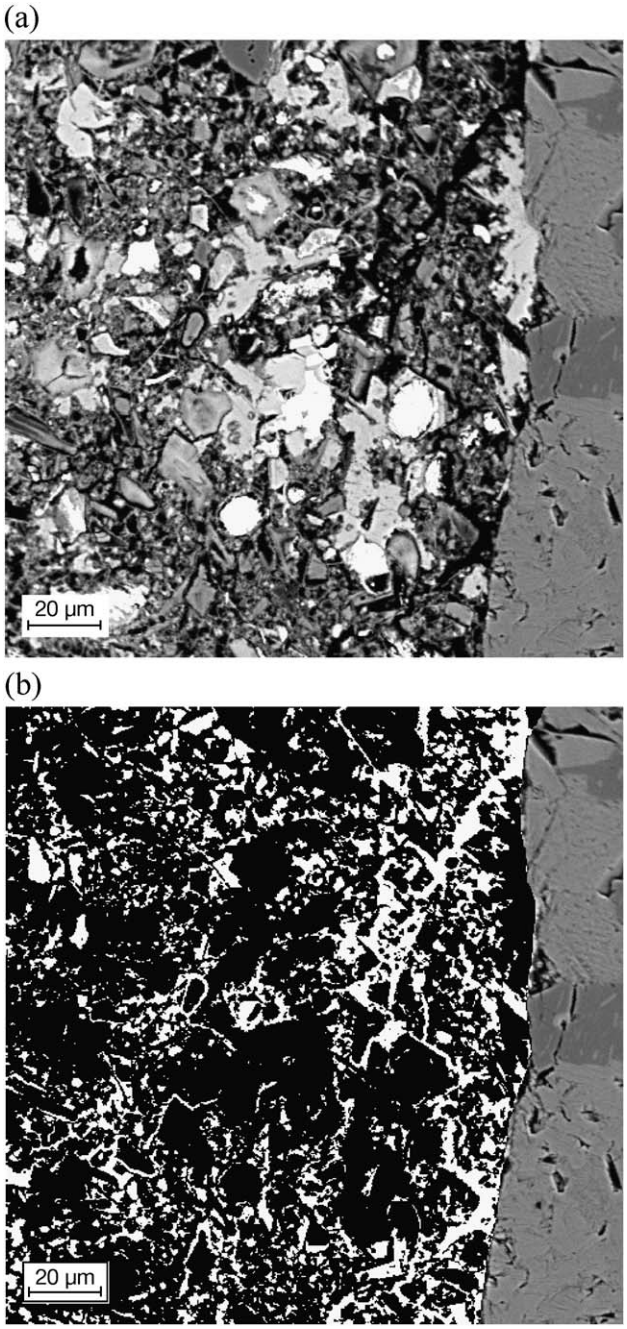

Fig. 2. (a) Paste around 2.36–4.75 mm aggregate in 7-day old mortar with w/c 0.55; (b) segmented pores around the aggregate shown in (a).

limits are valid for all of images processed. Based on the grey level limits obtained from the preliminary analysis the segmentation process was carried out by applying the same limits to all images. Fig. 2 shows the segmented pores around aggregate particle in 7-day old mortar with w/c of 0.55. In order for the specific feature to be included in the count it had to have a minimum dimension of 1 pixel (0.34 μm). Thus, the results presented here are for the detectable features and do not represent the absolute values. The area fraction of each feature was obtained and used as a basis for the characterization of the ITZ microstructure.

The values of porosity and UH content obtained from the bulk paste images, which had dimensions of 175 × 175 μm, were compared to those obtained from the 10-μm strips representing the ITZ. The effect of the image size on the results of the image analysis was examined by selecting two bulk paste images randomly from the pool of the bulk paste images and dividing them into 10-μm strips. The values of the feature's area fraction obtained from these strips were averaged and compared to the value obtained from the entire image. The results of the image analysis of the two bulk paste images and the 10-μm strips cut from them are given in Table 2. The results demonstrate that the average porosity and UH content obtained from the 10-μm strips are very close to the values obtained from the 175 × 175-μm image. Thus, the image size appears not to affect the results based on the range of image sizes analyzed above. The BSE images for the two bulk paste fields are shown in Fig. 3. The values of the porosity and the UH content for all the 10-μm strips from the bulk paste image corresponds to field 1 are provided in Fig. 4a and b.

The results of image analysis are presented in Figs. 5–8. Fig. 5 shows the variation in detectable porosity with the distance from the aggregate surface for the two aggregate sizes analyzed for mortar with w/c of 0.55 at 7 and 180 days as well as the bulk paste porosity, which is represented by points outside the *x*-scale range of the graph. Fig. 6 shows the change in the UH content with the distance from the aggregate surface and the UH content of the bulk paste for the same mortar and time periods as previously shown in Fig. 5. Fig. 7 depicts the ITZ and bulk paste porosity for mortar with w/c 0.40 at 7 and 180 days. The variation in UH content with the distance from the aggregate surface along with the UH content of the bulk paste for w/c 0.40 is shown in Fig. 8. The porosity and the UH content per strip are assumed to be concentrated in the middle of the strip to illustrate the variation in both quantities as a function of the distance away from the aggregate surface.

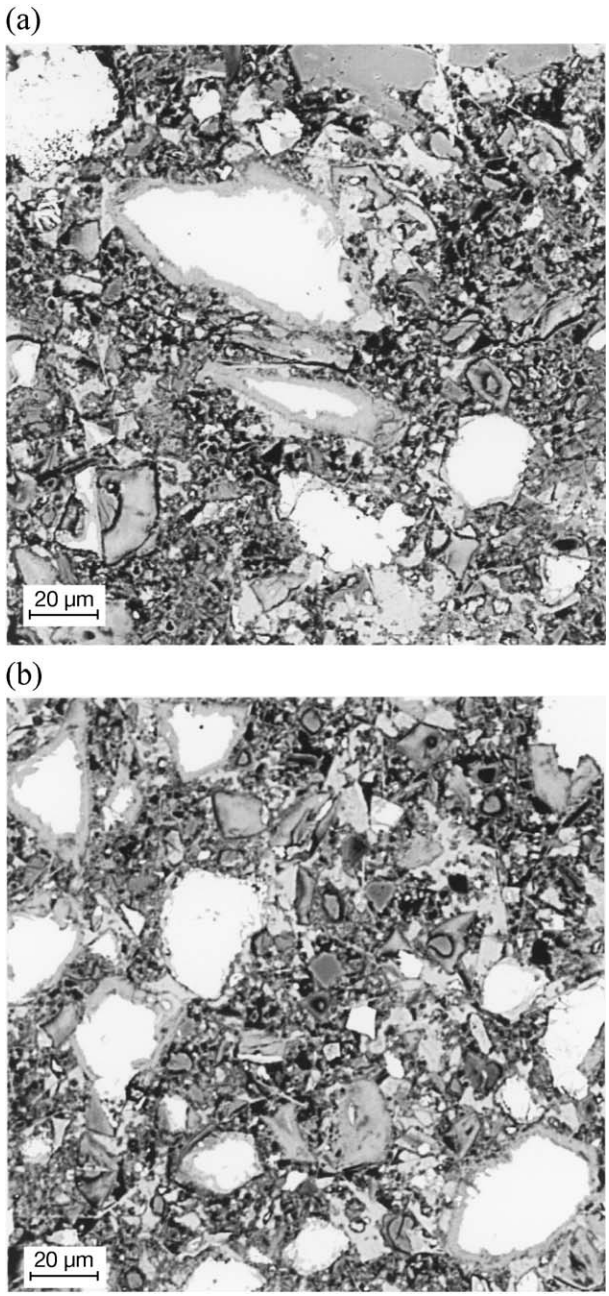

Fig. 3. (a) BSE image of bulk paste field 1; (b) BSE image of bulk paste field 2.

Table 2
Comparison of the image analysis results obtained from the 175 × 175-μm bulk paste images and the average of 10-μm strips cut from the same image

	Field 1		Field 2	
	Entire field	10-μm strips	Entire field	10-μm strips
Detectable porosity (%)	13.25	12.86	10.66	10.34
UH (%)	16.96	19.35	16.95	19.43

3. Discussion and analysis

3.1. Aggregate size effect

As shown in Fig. 5, at w/c of 0.55 the ITZ associated with 2.36- to 4.75-mm (#4–8) aggregate size has a higher porosity than the one surrounding 150- to 300-μm (#50–100) aggregate size at both 7 and 180 days. The porosity

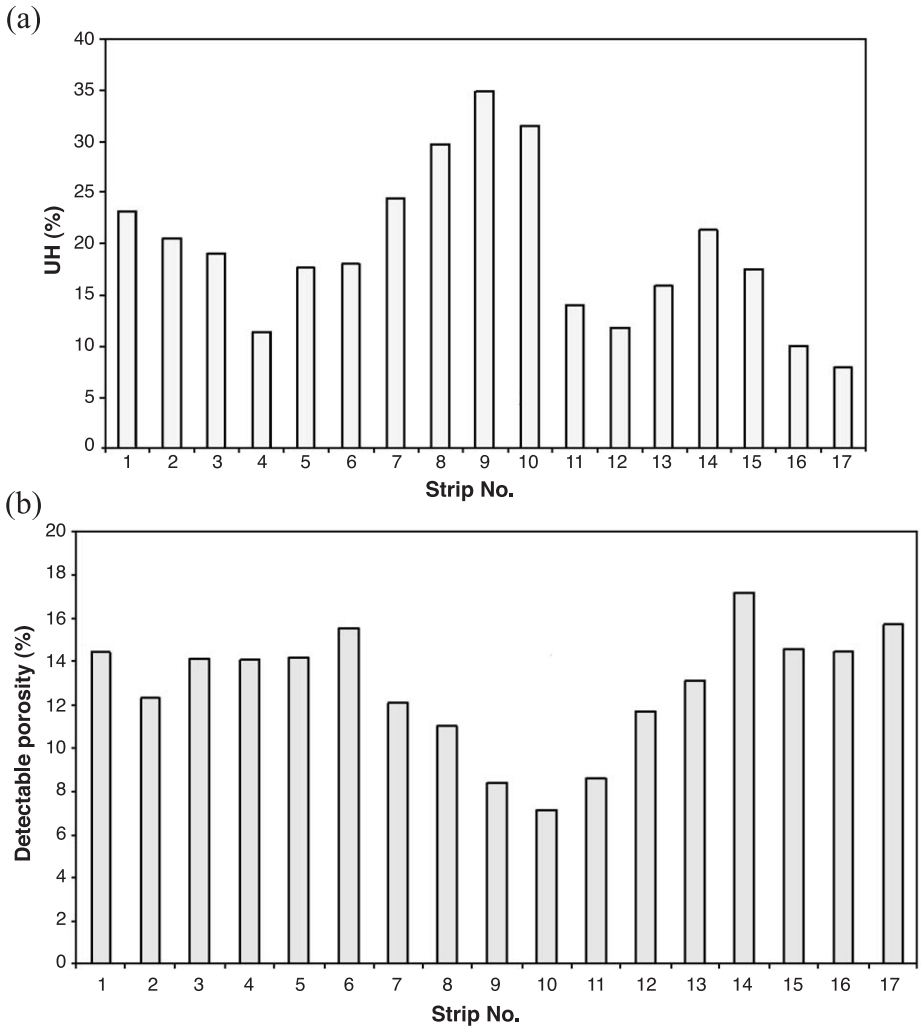

Fig. 4. (a) UH content of the bulk paste as given by 10-μm strips for field 1; (b) detectable porosity of the bulk paste as given by 10-μm strips for field 1.

curves for the two aggregate sizes seem to merge at the distance of about 35 μm away from the aggregate surface. At the age of 180 days, the two aggregate sizes appear to have equal porosity in the first 10-μm strip. Beyond that paste surrounding 150- to 300-μm aggregate seems to have lower porosity than paste surrounding 2.36- to 4.75-mm aggregate. The ITZ thickness can be estimated by extending the porosity curves until they intersect with the porosity of the bulk paste. Based on this procedure ITZ thickness for 150- to 300-μm aggregate size appears to be around 40 μm at both 7- and 180-day ages. As for 2.36- to 4.75-mm aggregate the ITZ thickness is estimated to be around 40 μm at 7-day age and around 50 μm at 180-day age.

The UH content in the ITZ and the bulk paste for w/c of 0.55 mortar is shown in Fig. 6. At 7 days, the ITZ around the 150- to 300-μm (#50–100) aggregate has a larger UH content than the ITZ around the 2.36- to 4.75-mm (#4–8) aggregate. The UH content around the 150- to 300-μm (#50–100) aggregate approaches that of the bulk paste at a distance of 25 μm from the aggregate surface while for the 2.36- to 4.75-mm (#4–8) aggregate the merging point with the bulk paste extends beyond 35 μm. At 180 days, the percentage of UH content in the ITZ for 150- to 300-μm aggregate size does not change much with distance away from the aggregate surface and there is no significant difference between the ITZ and the bulk paste at this age. As for 2.36- to 4.75-mm aggregate the UH content is lower than that of the 150- to 300-μm aggregate at the distance of 5 and 15 μm from the aggregate surface. For the rest of the strips there is no difference in UH content between the two aggregate sizes.

For w/c of 0.40 (Fig. 7), the ITZ porosity for the two aggregate sizes is similar in the first two strips surrounding the aggregate at the 7 days. However, at the same age the 2.36- to 4.75-mm aggregate appears to have less porosity for strips located 25 and 35 μm away from the surface of the aggregate than 150- to 300-μm aggregate. The ITZ thickness is estimated to be about 35 μm for 2.36- to 4.75-mm aggregate. As for 150- to 300-μm aggregate the ITZ thickness can be estimated to be around 40 μm based on the gradient of the porosity curve for the first three points. At 180 days, the ITZ around 150- to 300-μm aggregate

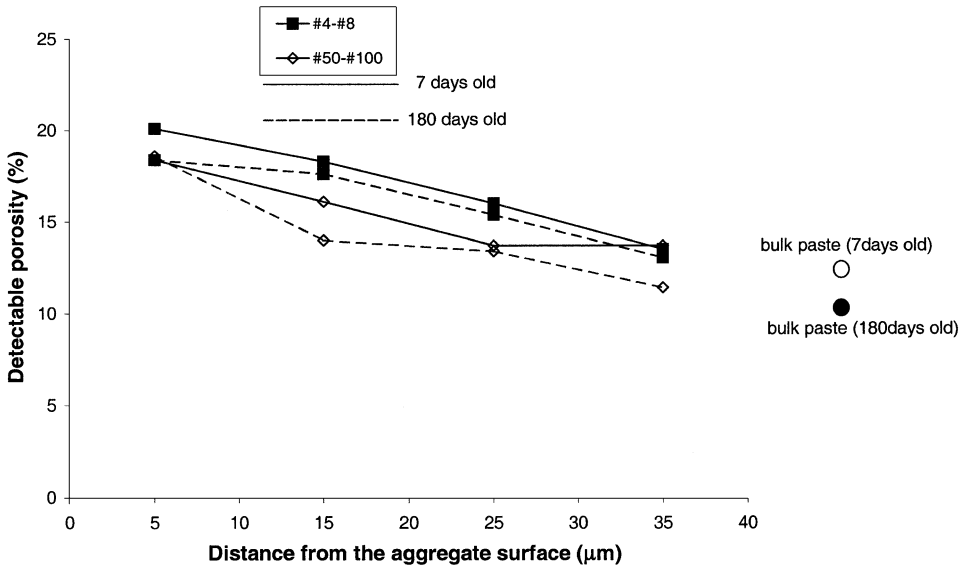

Fig. 5. Percent of detectable porosity in the successive 10-μm-wide strips around the aggregate and bulk paste for mortar with w/c of 0.55.

becomes less porous than the one surrounding the 2.36- to 4.75-mm aggregate. At this w/c and age the thickness of the ITZ around 150- to 300-μm aggregate appears to be reduced to 10 μm, while for 2.36- to 4.75-mm aggregate the ITZ thickness appears to be around 40 μm.

At 7 days, the ITZ around the 150- to 300-μm (#50–100) aggregate has a higher UH content than the ITZ around 2.36- to 4.75-mm (#4–8) aggregate as shown in Fig. 8. The UH content around the 150- to 300-μm (#50–100) aggregate approaches the level of the bulk paste at 25 μm while for 2.36- to 4.75-mm (#4–8) aggregate the UH merging point with the bulk paste extends beyond 35 μm. At 180 days, the difference in UH content between the two aggregate sizes becomes smaller. The UH content around 150- to 300-μm aggregate reaches the bulk paste level at 20 μm from the aggregate surface while the UH content around 2.36- to 4.75-mm aggregate approaches the bulk paste UH content at 30 μm from the aggregate surface.

The results discussed above reveal the effect of the aggregate size on the ITZ microstructure. It appears that reducing the aggregate size leads to lower porosity and higher UH content in the ITZ. The effect of aggregate size on the ITZ microstructure may be explained as follows: a large aggregate particle tends to accumulate more bleed water around it than the smaller aggregate particle. This could lead to a higher local w/c around the large aggregate

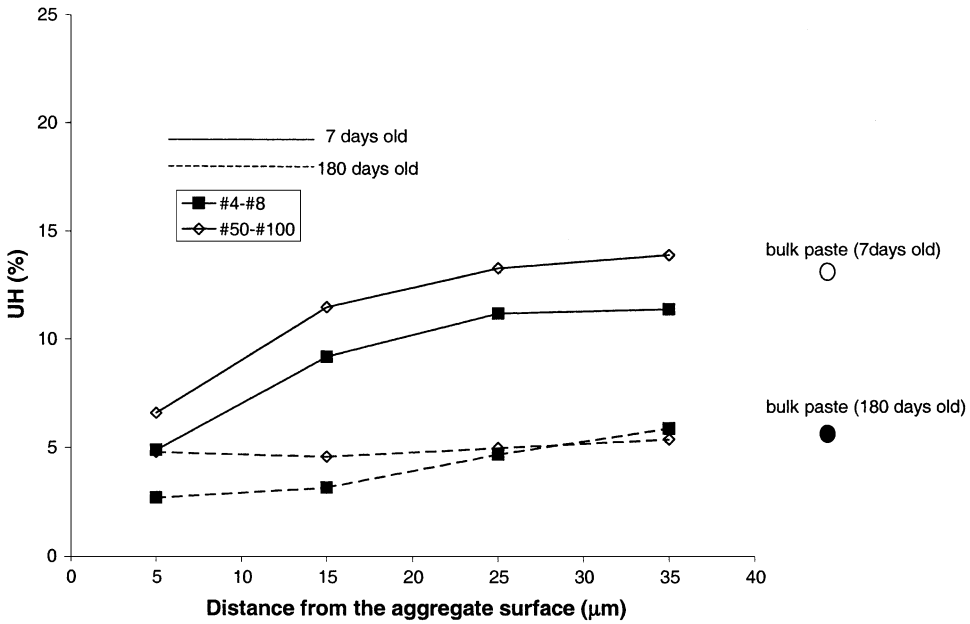

Fig. 6. Percent of UH in the successive 10-μm-wide strips around the aggregate and bulk paste for mortar with w/c of 0.55.

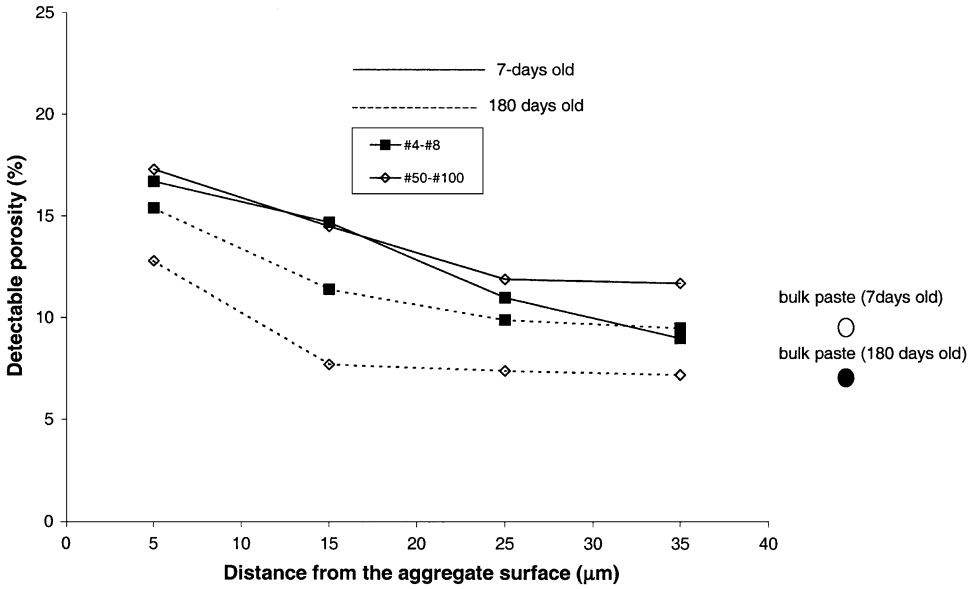

Fig. 7. Percent of detectable porosity in the successive 10-μm-wide strips around the aggregate and bulk paste for mortar with w/c of 0.40.

particle than around the small one. Subsequently, the ITZ for the large aggregate will contain a smaller amount of UH and a higher porosity than the ITZ around the small aggregate.

3.2. Effect of W/C

The influence of w/c on the ITZ microstructure and thickness was examined by comparing the porosity and the UH content of the ITZ for w/c of 0.55 and 0.40 mortars. In order to get a meaningful comparison, the porosity and UH content of the successive 10-μm strips were normalized with respect to those of the bulk paste. The normalization was achieved by dividing the value of the porosity or the UH content for any strip by the corresponding bulk paste value. As a result, the normalized value is the ratio between the ITZ and bulk paste porosity and UH content.

The normalized porosity for the successive 10-μm strips around the 2.36- to 4.75-mm (#4–8) aggregate corresponding to w/c 0.55 and 0.40 at 180–day age is shown in Fig. 9. The porosity in the 10-μm strip in the immediate vicinity of the aggregate appears to increase with reduction in the w/c ratio and is higher for w/c of 0.40 than that of 0.55. The subsequent strips show that the effect of w/

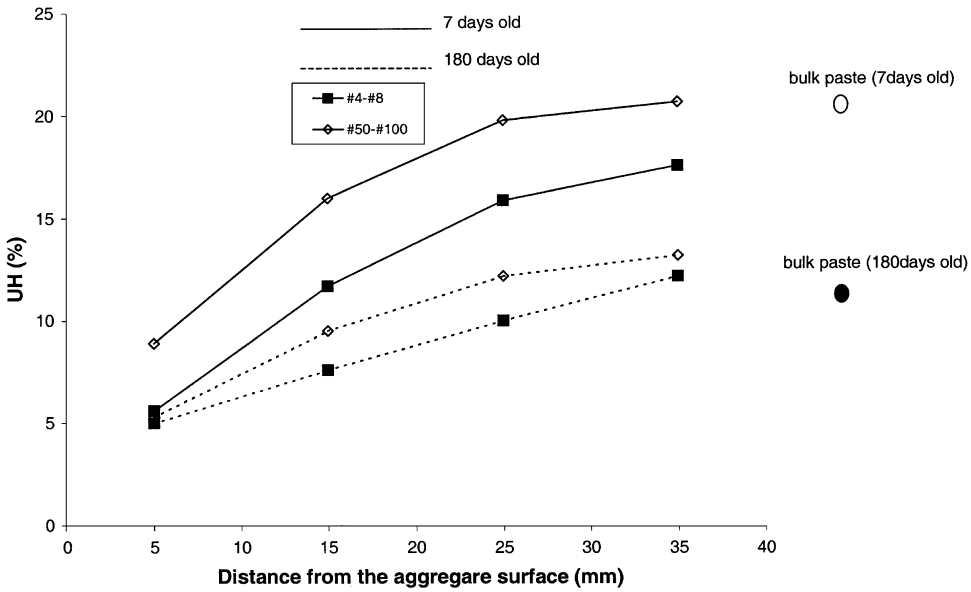

Fig. 8. Percent of UH in the successive 10-μm-wide strips around the aggregate and bulk paste for mortar with w/c of 0.40.

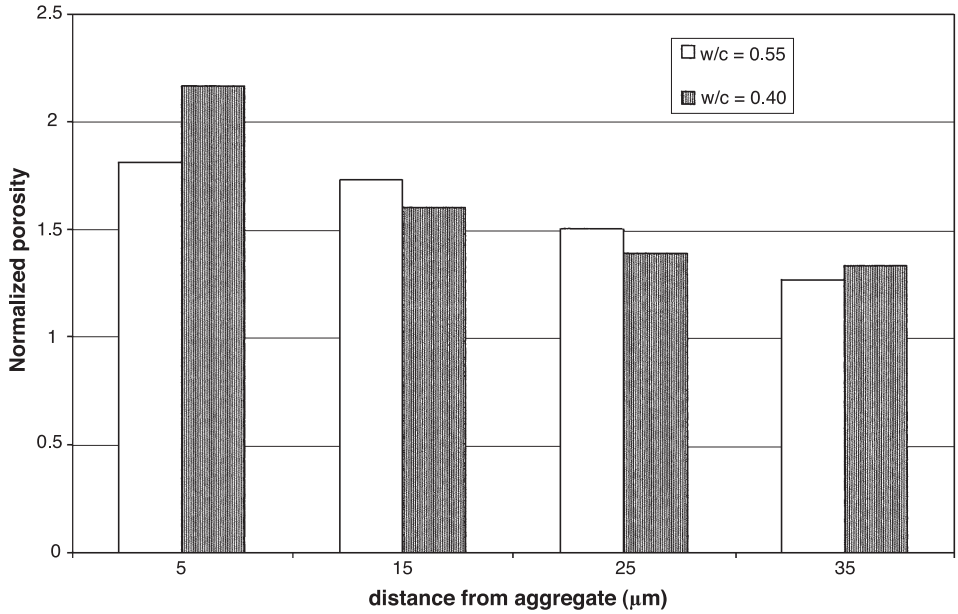

Fig. 9. Normalized porosity of successive 10-μm-wide strips around #4–8 aggregate in mortars specimens with w/c of 0.55 and 0.40 at 180 days.

c on the ITZ is modest for this aggregate size, as the normalized porosity for w/c 0.55 is slightly larger than that of 0.40.

The normalized porosity of the successive 10-μm strips around the 150- to 300-μm (#50–100) aggregate with w/c of 0.55 and 0.40 at 180 days is shown in Fig. 10. Comparing these data with the set of data from Fig. 9 it appears that the reduction of the w/c has a more pronounced effect on the normalized porosity for the 150- to 300-μm (#50–100) aggregate than for the 2.36- to 4.75-mm (#4–8) aggregate. For all of the strips illustrated in Fig. 10 the normalized porosity of mortar prepared with w/c of 0.40 is lower than that of mortar with w/c of 0.55, although for the first strip the difference is insignificant. It appears that the thickness of the ITZ around 150–300 μm aggregate for mortar with w/c of 0.40 is not larger than 10 μm. The porosity at distances greater than 10 μm from the surface of the aggregate is the same as the porosity of the bulk paste. For mortar made with w/c of 0.55 the porosity of successive 10-μm strips is higher than that of the bulk paste all the way from the aggregate surface up to 35 μm. The reduction of the w/c from 0.55 to 0.40 seems to reduce the ITZ thickness by at least 75%, but

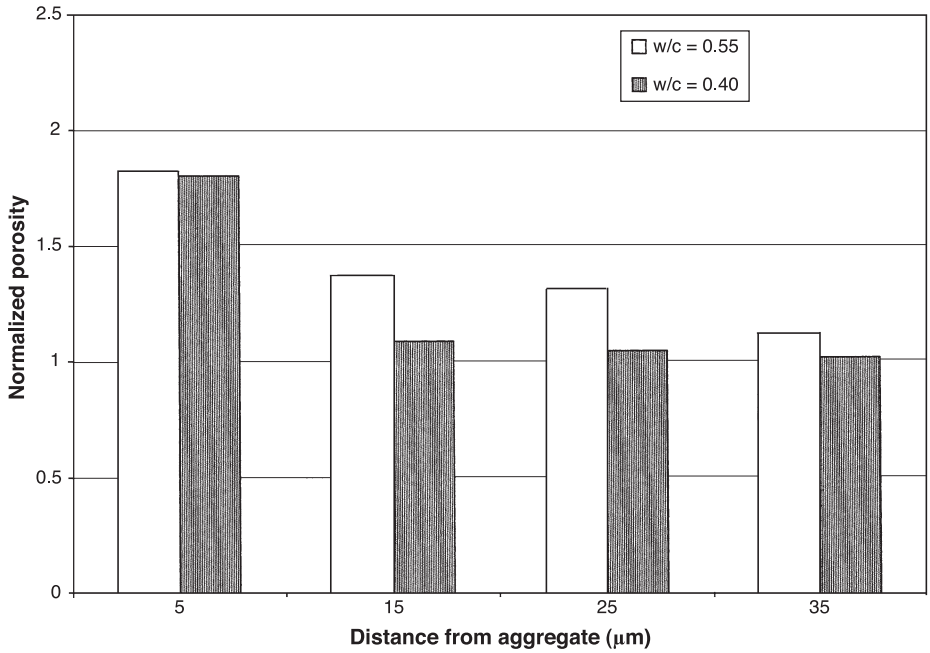

Fig. 10. Normalized porosity of successive 10-μm-wide strips around #50–100 aggregate in mortars specimens with w/c of 0.55 and 0.40 at 180 days.

it does not appear to have an influence on the normalized porosity of the 10-μm strip in the immediate vicinity of the aggregate.

The normalized UH content of the successive 10-μm strips around the 150- to 300-μm (#50–100) aggregate with w/c of 0.55 and 0.40 at 7 and 180 days is shown in Fig. 11a and b, respectively. At 7 days, the normalized UH content in the successive 10 μm strips for w/c of 0.55 and 0.40 follow the same trend. The normalized UH content increases from about 0.50 in the 10-μm strip surrounding the aggregate to a value equal to one at 25 μm away from the aggregate surface. At 180 days (Fig. 11b), the normalized UH content for w/c 0.55 is almost the same for all strips. Thus, the ITZ and the bulk paste have almost the same UH contents at this age. Based on the UH content at 7 and 180 days this may suggest that for w/c of 0.55, more cement grains hydrated in the bulk paste than in the ITZ and more hydration products are deposited there in the period between 7 and 180 days. Consequently, the bulk paste porosity will be considerably reduced as compared to the ITZ. As for w/c of 0.40, at 180 days (Fig. 11b), the normalized UH content gradient is similar to that at 7 days.

The results discussed in this section suggest that the w/c has an influence on the ITZ microstructure and thickness. However, this influence appears to depend on the aggregate size. Reducing the w/c from 0.55 to 0.40 almost eliminated

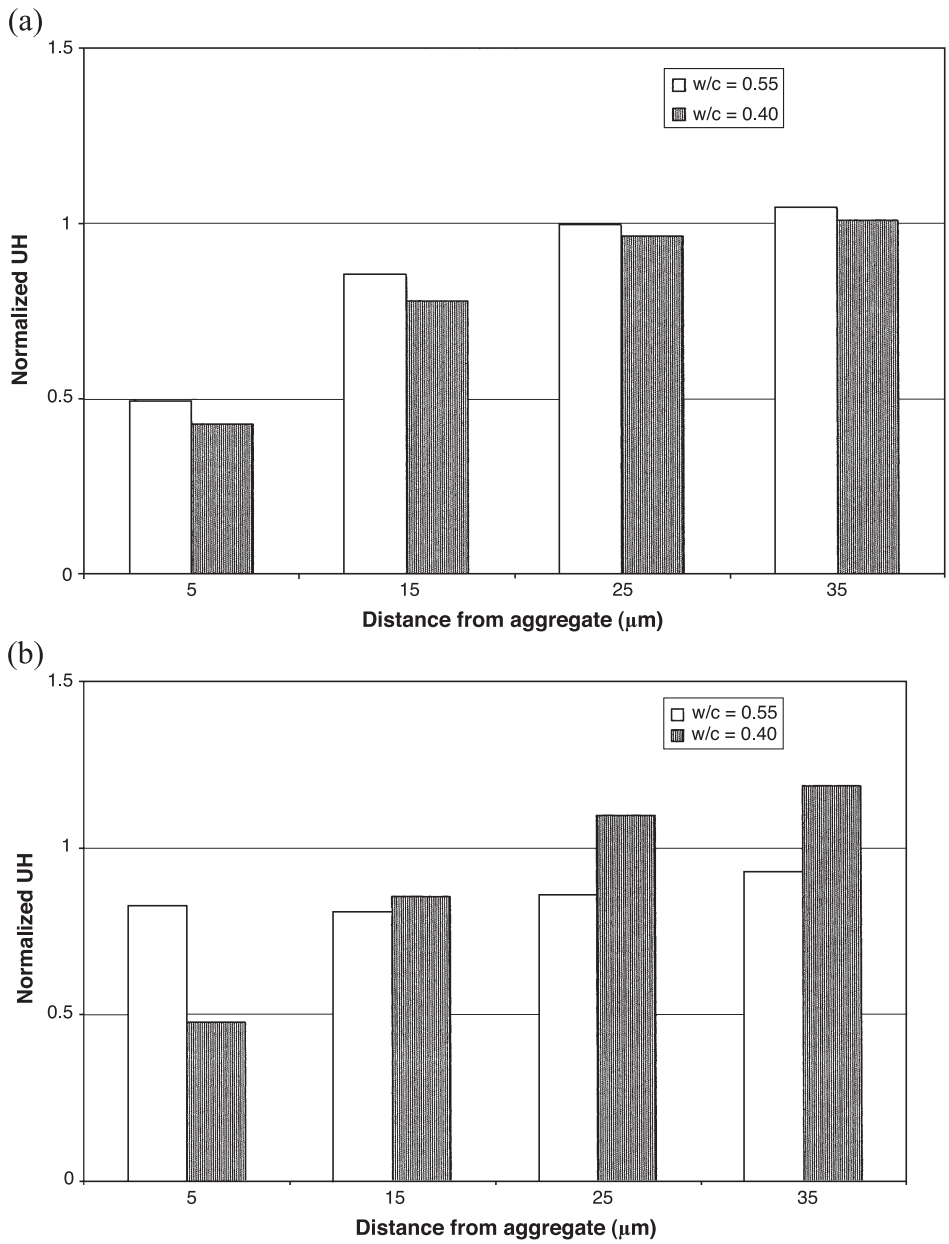

Fig. 11. (a) Normalized UH content for successive 10-μm-wide strips around #50–100 aggregate in mortar with w/c of 0.55 and 0.40 at 7 days; (b) normalized UH content for successive 10-μm-wide strips around #50–100 aggregate in mortar with w/c of 0.55 and 0.40 at 180 days.

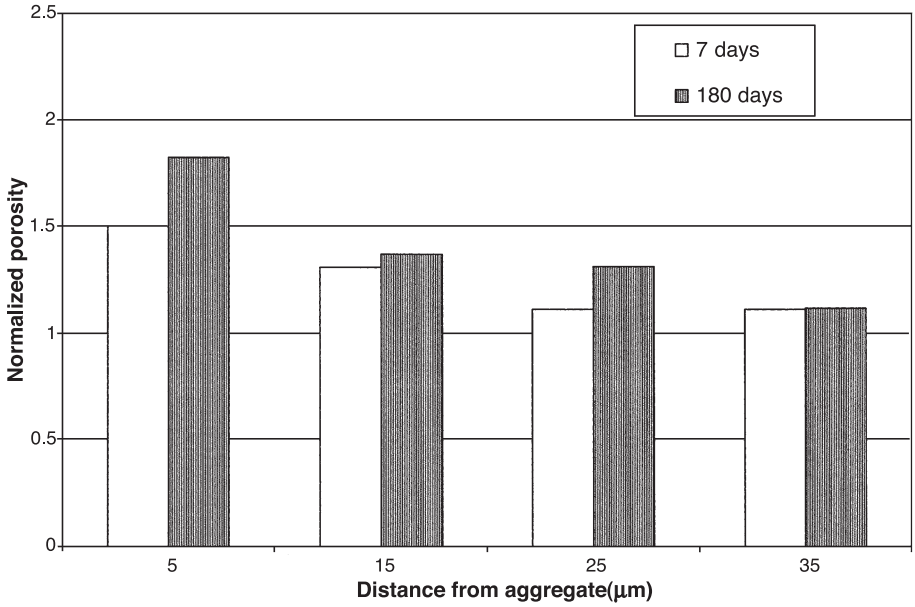

Fig. 12. Normalized porosity for successive 10-μm-wide strips around #50–100 aggregate in mortar specimens with w/c of 0.55.

the ITZ for the 150- to 3000-μm (#50–100) aggregate particles as demonstrated above. As for the 2.36- to 4.75-mm (#4–8) aggregate particle the effect of reducing w/c on the normalized porosity of the ITZ appears to be minor. At the age of 7 days, the UH content in the ITZ relative to that of the bulk paste is independent of the w/c for 150- to 300-μm (#50–100) aggregate particles. At the age of 180 days, the UH content in the ITZ for w/c of 0.55 is almost the same as that of the bulk paste, while for w/c of 0.40 the UH content of the ITZ relative to the bulk paste appears to have the same gradient as at 7-day age.

3.3. Age effect

The concept of normalized porosity is used to study the effect of age on the microstructure of the ITZ and the bulk paste. The normalized porosity for successive 10-μm strips around 150- to 300-μm (#50–100) aggregate and the 2.36- to 4.75-mm (#4–8) aggregate with w/c of 0.55 at 7 and 180 days is shown in Figs. 12 and 13, respectively. The trend observed for both aggregate sizes suggests that the normalized porosity increases with the increase in the curing time. At first this may seem contradictory to the common con-

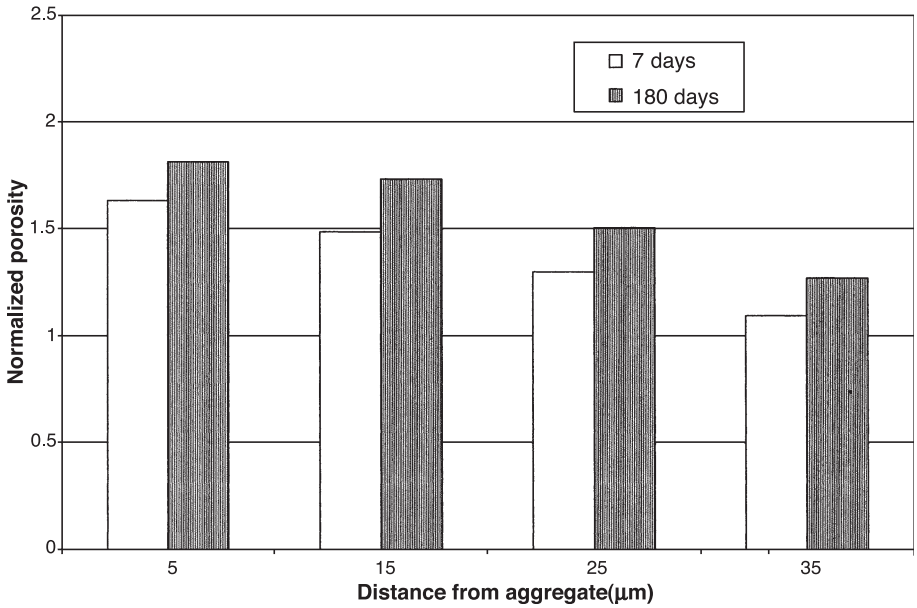

Fig. 13. Normalized porosity for successive 10-μm-wide strips around #4–8 aggregate in mortar specimens with w/c of 0.55.

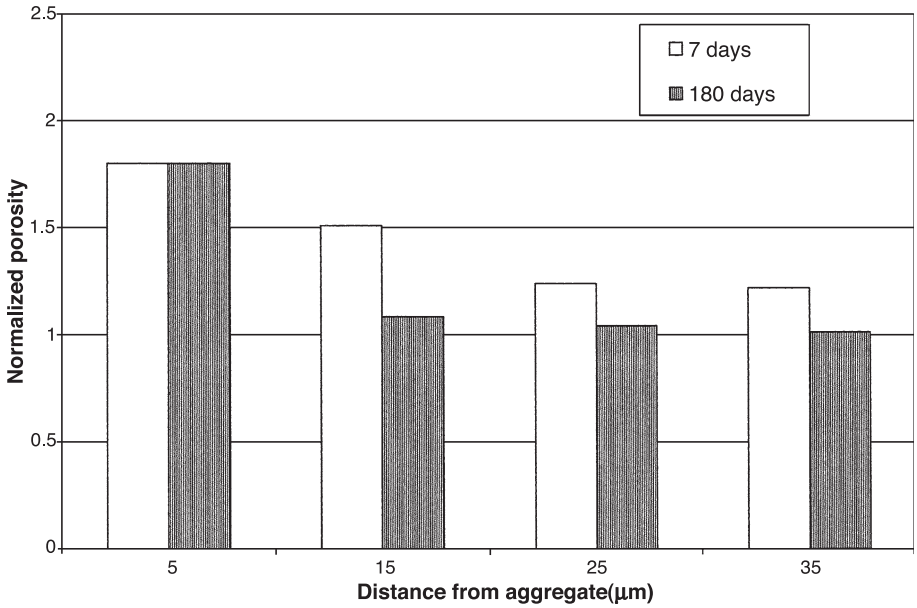

Fig. 14. Normalized porosity for successive 10-μm-wide strips around #50–100 aggregate in mortar specimens with w/c of 0.40.

ception that the porosity of the ITZ should be reducing with time. This seemingly conflicting result can be explained as follows: at the age of 7 days, the ITZ has a lower UH content than the bulk paste, but at 180 day age both have the almost the same UH content as has been demonstrated in the previous section and shown in Fig. 6. This suggests that longer curing period resulted in more cement grains hydrating in the bulk paste than in the ITZ and, hence, the bulk paste porosity was reduced at a higher rate than that of the ITZ. As a result the ratio between the porosity of the ITZ and the bulk paste increased with time.

The effects of age for the 150- to 300-μm (#50–100) aggregate and the 2.36- to 4.75-mm (#4–8) aggregate at w/c of 0.40 are shown in Figs. 14 and 15, respectively. At this w/c the trend is reversed for the 150- to 300-μm (#50–100) aggregate as compared to those observed for w/c of 0.55. The normalized porosity of the successive 10-μm strips is reduced with time as seen in Fig. 14. This reversed trend can be explained by the presence of sufficient UH content within layers close to aggregate surface to densify the microstructure with time. As for the 2.36- to 4.75-mm (#4–8) aggregate (Fig. 15), normalized porosity increases

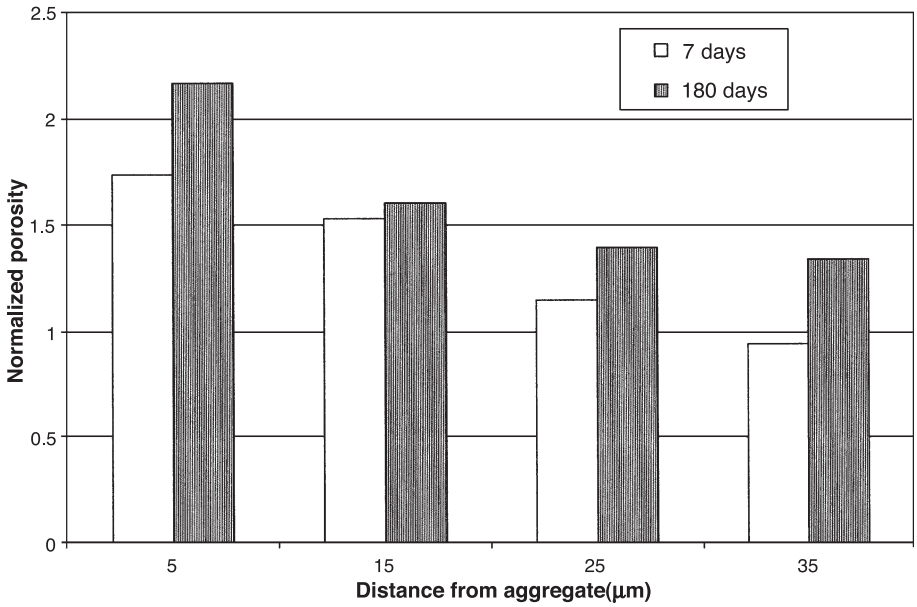

Fig. 15. Normalized porosity for successive 10-μm-wide strips around #4–8 aggregate in mortar specimens with w/c of 0.40.

with time. This can be attributed to the presence of smaller amount of UH in the successive 10-μm strips around the 2.36- to 4.75-mm (#4–8) aggregate at the 7-day age as compared to the 150- to 300-μm (#50–100) aggregate, as shown in Fig. 8.

The results presented in this section suggest that age effect on the ITZ normalized porosity depends on its initial microstructure. The amount of the UH present in the ITZ at early age controls the microstructure at later age. The amount of UH in the area surrounding the aggregate appears to depend on the aggregate size and the w/c. Thus, these two factors may be considered as controlling parameters influencing the evolution of the ITZ with time.

4. Conclusions

The effect of aggregate size, w/c, and aging on the ITZ microstructure has been investigated. The following conclusions are drawn from the investigation:

1. At the same w/c and age, reducing the aggregate size from 2.36–4.75 mm range to 150–300 μm range tends to reduce the porosity and increase the content of unhydrated particles (UH) in the region surrounding the aggregate.
2. Within the range of w/c studied, the results suggest that reducing the w/c from 0.55 to 0.40 appears to reduce the porosity of the successive 10-μm strips surrounding 150- to 300-μm aggregate. As for successive 10-μm strips surrounding 2.36- to 4.75-mm aggregate the effect of reducing w/c on porosity appears to be insignificant.
3. The results indicate that the evolution of the ITZ microstructure with time depends on its initial microstructure. For w/c 0.55, between 7 and 180 days, the ITZ appears to develop more porous microstructure relative to that of the bulk paste. This is perhaps due to the deficiency in the UH content in the ITZ as compared to the bulk paste at an early age. For w/c 0.4, between 7 and 180 days, the ITZ surrounding 150- to 300-μm aggregate appears to develop denser microstructure relative to that of the bulk paste. This may be attributed to the presence of relatively high amount of UH in the ITZ at an early age, which will eventually fill the pores with hydration products at a later age.
4. The effect of the aggregate size on the ITZ thickness does not seem to be following specific trend and appears to depend on the feature used to define the ITZ thickness. If the ITZ thickness is based on porosity gradient, reduction of the aggregate size appears to reduce the ITZ thickness to only 10 μm for mortar prepared with w/c of 0.40 and cured for 180 days. For mortar with the same w/c, but cured for only 7 days as well as for mortar with w/c of 0.55 cured for 7 and 180 days, reduction of the aggregate size does not seem to reduce the ITZ thickness as based on porosity gradient. For ITZ thickness based on UH content reducing the aggregate size tends to reduce the ITZ thickness for mortars with w/c of 0.55 and 0.40 cured for 7 days. At 180-day age the effect of the aggregate size on ITZ thickness based on UH content appears to be insignificant.

Appendix A. Determination of the number of images

Assuming normal distribution for the sample, the following equation can be used

$$Z = \frac{\bar{X} - \mu_o}{\frac{S}{\sqrt{n}}} \quad (1)$$

Where Z = standard normal variable; $\bar{X}$ = Average obtained from the image analysis; μ_o = true average; S = standard deviation; n = number of images.

For 95% confidence interval Z is equal 1.96 as given by the standard normal distribution tables. The number of images required to approach a difference of □ between the calculated and true averages can be given by substituting the value of Z corresponding to 95% confidence in Eq. (1) and rearrange the equation as shown below

$$n = \left[\frac{1.96S}{\delta}\right]^2 \quad (2)$$

The number of images required for the 10-μm strips surrounding the aggregate can be determined by using the average and standard deviation for the porosity and UH obtained from 100 images in the preliminary analysis stage. The value selected for δ is 10% of the average. The larger value of n is used as the basis for the required number of images as shown below for #4–8 aggregate at 7-day age:

Average UH = 4.95%	Average porosity = 20%
Standard deviation = 2.3%	Standard deviation = 10.4%
n = 84	n = 103

References

[1] K.L. Scrivener, A. Bentur, P.L. Pratt, Quantitative characterization of the transition zone in high strength concretes, Adv. Cem. Res. 1 (1988) 230–237.
[2] P.J.M. Monteiro, J.C. Maso, J.P. Ollivier, The aggregate–mortar interface, Cem. Concr. Res. 15 (6) (1985) 953–958.
[3] K.O. Kjellsen, O.H. Wallevik, L. Fjalberg, Microstructure and microchemistry of the paste–aggregate interfacial transition zone of high performance concrete, Adv. Cem. Res. 10 (1998) 33–40.
[4] K.L. Scrivener, P.L. Pratt, Characterization of interfacial microstructure, in: J.C. Maso (Ed.), Interfacial Transition Zone in Concrete, RILEM Report, vol. 11, E & FN Spon, London, 1996, pp. 3–17.
[5] A. Bentur, I. Odler, Development and nature of interfacial microstructure, in: J.C. Maso (Ed.), Interfacial Transition Zone in Concrete, RILEM Report, vol. 11, E & FN Spon, London, 1996, pp. 18–44.

[6] K.L. Scrivener, Characterization of the ITZ and its quantification by test method, in: M.G. Alexander, G. Arlliguie, G. Ballivy, A. Bentur, J. Merchand (Eds.), Engineering and Transport Properties of the Interfacial Transition Zone in Cementitious Composites, RILEM Report, vol. 20, RILEM Publications, 1999, pp. 3–14.
[7] A. Bentur, M.G. Alexander, A review of the work of the RILEM TC159-ETC: Engineering of the interfacial transition zone in cementitious composites, Mat. Struct. 33 (2000) 82–87.
[8] X. Ping, J.J. Beaudoin, R. Brousseau, Effect of the aggregate size on transition zone properties at the Portland cement paste interface, Cem. Concr. Res. 21 (1991) 999–1005.
[9] S. Diamond, J. Huang, The ITZ in concrete—A different view based on image analysis and SEM observations, Cem. Concr. Compos. 23 (2001) 179–188.
[10] S. Diamond, Considerations in image analysis as applied to investigations of the ITZ in concrete, Cem. Concr. Compos. 23 (2001) 171–178.